Smart Structures and Systems, *Vol. 16, No. 1 (2015) 223-242*
DOI: http://dx.doi.org/10.12989/sss.2015.16.1.223

Damage detection on a full-scale highway sign structure with a distributed wireless sensor network

Zhuoxiong Sun*[1], Sriram Krishnan[1], Greg Hackmann[2], Guirong Yan[3], Shirley J. Dyke[1,4], Chenyang Lu[2] and Ayhan Irfanoglu[4]

[1]*School of Mechanical Engineering, Purdue University, USA*
[2]*Department of Computer Science and Engineering, Washington University in St. Louis, USA*
[3]*Department of Civil Engineering, University of Texas at El Paso, USA*
[4]*School of Civil Engineering, Purdue University, USA*

(Received January 27, 2014, Revised July 25, 2014, Accepted March 9, 2015)

Abstract. Wireless sensor networks (WSNs) have emerged as a novel solution to many of the challenges of structural health monitoring (SHM) in civil engineering structures. While research projects using WSNs are ongoing worldwide, implementations of WSNs on full-scale structures are limited. In this study, a WSN is deployed on a full-scale 17.3m-long, 11-bay highway sign support structure to investigate the ability to use vibration response data to detect damage induced in the structure. A multi-level damage detection strategy is employed for this structure: the Angle-between-String-and-Horizon (ASH) flexibility-based algorithm as the Level I and the Axial Strain (AS) flexibility-based algorithm as the Level II. For the proposed multi-level damage detection strategy, a coarse resolution Level I damage detection will be conducted first to detect the damaged region(s). Subsequently, a fine resolution Level II damage detection will be conducted in the damaged region(s) to locate the damaged element(s). Several damage cases are created on the full-scale highway sign support structure to validate the multi-level detection strategy. The multi-level damage detection strategy is shown to be successful in detecting damage in the structure in these cases.

Keywords: multi-level damage detection; full scale structure; wireless sensor network

1. Introduction

Civil engineering structures such as bridges will suffer from environmental corrosion, wind loading and traffic impact in their lifetime. Monitoring the condition of these structures is important for prioritizing repair and replacement of our inventory and even for protecting structures from collapse or accelerated deterioration. Monitoring using distributed wireless sensor networks (WSNs) has become a novel and promising solution to the challenges of structural health monitoring (SHM) in civil engineering structures (Xu *et al.* 2004, Chintalapudi *et al.* 2006, Lynch and Loh 2006, Kim *et al.* 2007 and Spencer and Yun 2010), such as bridges, buildings and highways.

WSNs have numerous advantages over traditional wired sensor networks. Installation and

*Corresponding author, Ph.D., E-mail: zxsun152@gmail.com

http://www.techno-press.org/?journal=sss&subpage=8 ISSN: 1738-1584 (Print), 1738-1991 (Online)

maintenance costs are considerably reduced and energy consumption is relatively low (Chintalapudi *et al.* 2006, Pakzad *et al.* 2008, Nagayama and Spencer 2008, Zimmerman *et al.* 2008). Also, the embedded computational capabilities of wireless sensors allow onboard evaluations which can reduce the amount of data transmitted through the network significantly (Ferrigno *et al.* 2005, He and Wu 2006, Hackmann *et al.* 2010, Hackmann *et al.* 2012) and, consequently, improve the damage detection efficiency.

Recently a number of efforts have been conducted using WSNs for SHM in civil engineering community. Researchers at Clarkson University have developed a wireless monitoring system for bridge condition assessment. In the hybrid wireless system, accelerometers are used to obtain dynamic characteristic of the structure, and strain sensors are employed for assessing load rating and static analysis. The performances of the system have been tested on a single-span bridge with 20 wireless sensor nodes (Gangone *et al.* 2009). Researchers at the University of Illinois at Urbana-Champaign have deployed a large scale WSN for SHM in the new Jindo Bridge in South Korea. This implementation is the first dense deployment of WSNs on a cable-stayed bridge in the world and the largest (in the sense of the number of wireless sensors deployed) of its kind for civil infrastructure to date (Spencer 2009). Researchers at the University of Michigan have validated three output-only modal identification methods (peak-picking, random decrement, and frequency domain decomposition) using a distributed WSN. Experimental validation has also been performed on the balcony of a historic theater in metropolitan Detroit (Zimmerman *et al.* 2008). Researchers at Lehigh University have proposed an iterative modal identification algorithm for SHM with WSNs. Onboard computational power of wireless nodes is utilized to reduce communication burden and energy consumption for modal identification tasks (Dorvash *et al.* 2013). Researchers at Georgia Institute of Technology have implemented a wireless mobile sensor network for system identification on a space-frame bridge. Four mobile wireless nodes navigate autonomously to different sections of the bridge for measuring vibrations. The mobile wireless system has been shown to provide consistent and reliable measurements (Zhu *et al.* 2012).

In the research efforts discussed above, the focus has been on the monitoring of real-world structures and use of modal identification with distributed WSNs, multi-hop communication or distributed modal identification algorithms validation. Because it is typically not permitted to damage a structure that is in service, none of these works studied damage detection algorithms validation. In this paper, a multi-level damage detection strategy is implemented on a full-scale sign support truss structure which was previously mounted over Inter-state I-29 near Sioux City in Iowa. The goals of this study are i) full implementation of the proposed multi-level damage detection strategy with distributed modal identification algorithm (frequency domain decomposition with peak-picking); ii) validation of the damage detection strategy on real world structure working with a dense array of wireless sensors; iii) evaluation of the capabilities of the damage detection strategy with several different damage scenarios.

2. Methodology

A multi-level damage detection strategy is studied for the truss structure in this work. For the multi-level detection strategy, a coarse resolution Level I detection is conducted first to detect damaged region(s) of the structure. Afterwards, a fine resolution Level II detection is applied to detect the damaged element(s) in the structure. The algorithms selected for the Level I and Level II use natural frequencies and mode shapes of a structure which can be obtained using output-only

modal identification algorithms with WSNs. The implementation of the damage detection strategy with WSNs is illustrated in Fig. 1. The details are provided in this section.

2.1 Modal identification

After collecting the raw acceleration data, modal identification is performed online to identify natural frequencies and mode shapes of the structure. Herein we implement frequency domain decomposition (FDD) (Brincker *et al.* 2001) with peak-picking (Zimmerman *et al.* 2008, Castaneda *et al.* 2009) on the WSN nodes for modal identification as shown in Fig. 1. For each wireless node, onboard processing is utilized. Fast Fourier transform (FFT) is applied to raw data. Then, amplitude spectral density (ASD) is obtained. Peak-picking is applied to the ASD to identify natural frequencies of the structure and associated complex FFT coefficients. For each mode, natural frequency and the associated real part and imaginary part of the peak are required.

At the manager node, the cross spectral density (CSD) matrix is assembled at each natural frequency based on the complex FFT coefficients from leaf nodes and singular value decomposition (SVD) is applied to the CSD matrix. The first column of the left singular value matrix is used to estimate the mode shape of the structure. Using this approach, the modal identification task can be distributed among the network. The natural frequencies and mode shapes from the manager node are sent to the base station for constructing flexibility matrices for multi-level damage detection. For instance, for a five leaf node network with sampling frequency 256 Hz and sampling time 100 seconds, the total raw data to the base station is 256*100*5 = 128000. With the strategy in Fig. 1, assuming the first 10 mode shapes are used. From each leaf node, 3*10 = 30 float numbers are sent to the manager node. For the manager node, (5+1)*10 = 60 float numbers are sent to the base station. This communication strategy is much more efficient than transmitting raw data to the base station for centralized post-processing. The power consumption is also greatly reduced since the wireless transmission using imote2 platform has been reduced. It is worth mentioning, based on our previous studies, wireless transmission is especially power consuming for imote2 platform (Hackmann *et al.* 2012).

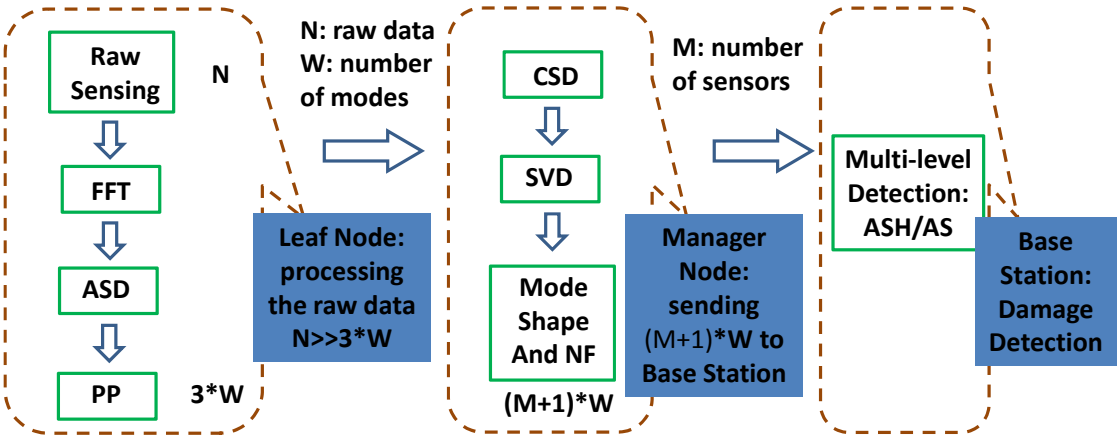

Fig. 1 Online sensing and damage detection implementation

2.2 Multi-level damage detection strategy

A multi-level damage detection strategy is employed for the implementation discussed herein. The multi-level damage detection strategy utilizes the modal properties of the structure for damage detection. The effectiveness of damage detection algorithms have been studied in previous researchers' work (Yan *et al.* 2011, Krishnan *et al.* 2011). Level I of damage detection uses the Angle-between-String-and-Horizon (ASH) flexibility-based algorithm (Yan *et al.* 2010). The structure is regarded as a beam-type structure, and only the vertical modes from either the top or bottom chord are used (i.e., vertical modes of leaf node sensors from 13 to 24 in Fig. 3(b)) to construct the ASH flexibility matrices before and after damage (see Eqs. (1) and (2)). The diagonal of ratio of ASH flexibility change (see Eq. (4)) in healthy and damaged cases is used to identify the damaged regions.

The r-th ASH mode shape R_r is given by

$$R_r = \left[\frac{1}{l_1}\varphi_{1,r} \quad \frac{1}{l_2}\left(\varphi_{2,r} - \varphi_{1,r}\right) \quad \cdots \quad \frac{1}{l_n}\left(\varphi_{n,r} - \varphi_{n-1,r}\right) \right]^T \tag{1}$$

where $\varphi_{i,r}$ is the i-th component of the r-th mode shape, l_i is the i-th beam length.

The ASH flexibility is given by

$$F_\theta = \sum_{r=1}^{n} \frac{1}{\omega_r^2} R_r R_r^T \tag{2}$$

where ω_r is the r-th circular natural frequency.

Then, the ratio of the ASH flexibility change is given by

$$R(\Delta F_\theta) = \left(F_\theta^d - F_\theta^u \right)./ F_\theta^u \tag{3}$$

where $F_\theta{}^d$ is the ASH flexibility matrix in the damaged case, $F_\theta{}^u$ is the ASH flexibility matrix in the undamaged or healthy case.

The absolute diagonal of ratio of change is given by

$$d(\Delta F_\theta) = \left| diag\left(R(\Delta F_\theta) \right) \right| \tag{4}$$

where $d(\Delta F_\theta)$ is used as the ASH damage indicator.

After identifying the regions of damage, sleeping sensors in that/those region(s) (i.e., the bay with damage) are woken up to perform a fine resolution, Level II damage detection using the Axial Strain (AS) flexibility based algorithm (Yan *et al.* 2009). In Level II of damage detection, the structure is regarded as a truss-type structure. Both vertical and horizontal modes along the length of the truss are used to construct the AS flexibility matrix (see Eqs. (5) and (6)) in the healthy and damaged cases (the AS flexibility matrix for the healthy case is constructed in advance and used as the baseline to compare with the damaged case AS flexibility matrix). The AS flexibility change (see Eq. (7)) is used as the damage indicator for Level II damage detection to identify which particular element is damaged.

The r-th AS mode shape S_r *is* given by

$$S_r = \begin{bmatrix} c_1 \dfrac{\left(\varphi_{2a-1,r} - \varphi_{2b-1,r}\right)}{l_1} + s_1 \dfrac{\left(\varphi_{2a,r} - \varphi_{2b,r}\right)}{l_1} \\ \cdots \\ c_j \dfrac{\left(\varphi_{2o-1,r} - \varphi_{2p-1,r}\right)}{l_j} + s_j \dfrac{\left(\varphi_{2o,r} - \varphi_{2p,r}\right)}{l_j} \\ \cdots \\ c_n \dfrac{\left(\varphi_{2w-1,r} - \varphi_{2x-1,r}\right)}{l_n} + s_n \dfrac{\left(\varphi_{2w,r} - \varphi_{2x,r}\right)}{l_n} \end{bmatrix} \tag{5}$$

where c_i and s_i are the cosine and sine values of angle between the i-th element and x and y global coordinate, respectively. l_i is the length of the i-th element.

The AS flexibility matrix is given by

$$F_{AS} = \sum_{r=1}^{n} \frac{1}{\omega_r^2} S_r S_r^T \tag{6}$$

where ω_r is the r-th circular natural frequency.

Then, the AS flexibility change is given by

$$\Delta F_{AS} = {F_{AS}}^d - {F_{AS}}^u \tag{7}$$

where ${F_{AS}}^d$ is the AS flexibility matrix in the damaged case and ${F_{AS}}^u$ is the AS flexibility matrix in the undamaged or healthy case.

The normalized AS flexibility change is given by

$$d(\Delta F_{AS}) = \left| diag\left({F_{AS}}^d - {F_{AS}}^u\right)\right| / \max\left| diag\left({F_{AS}}^d - {F_{AS}}^u\right)\right| \tag{8}$$

where $d(\Delta F_{AS})$ is used as the AS damage indicator.

3. Numerical simulation

A finite element model (FEM) of the full scale truss structure (Fig. 2) is built using Matlab to perform numerical evaluation of the damage detection strategy. The FEM model has 48 nodes and 144 elements. Each node has six degrees of freedom (DOFs). Beam elements and consistent mass matrices are used for the FEM model (see Fig. 3(a)).

3.1 Simulation of the experimental implementation

To simulate damage in the numerical study, Young's modulus is reduced by 50% in the damaged elements. It should be noted that damage simulated in this way may not be the same as the real damage on the structure. Then stiffness matrices [***K***] and mass matrices [***M***] from the FEM model with and without damaged elements are extracted for the equations of motion (EOM) of the

system (see Eq. (9)) to simulate shaker tests of the structure in damaged and healthy conditions. Rayleigh damping is used in the simulation. The EOM of the system is given by

$$\boldsymbol{M}\ddot{\boldsymbol{x}}+\boldsymbol{C}\dot{\boldsymbol{x}}+\boldsymbol{K}\boldsymbol{x}=\boldsymbol{F} \tag{9}$$

where $\boldsymbol{M}\in\boldsymbol{R}^{n\times n}$, $\boldsymbol{K}\in\boldsymbol{R}^{n\times n}$, $\boldsymbol{C}\in\boldsymbol{R}^{n\times n}$, $\boldsymbol{F}\in\boldsymbol{R}^{n\times 1}$. The state space form of Eq. (9) is given in Eqs. (10) and (11).

$$\begin{bmatrix}\dot{\boldsymbol{x}}\\ \ddot{\boldsymbol{x}}\end{bmatrix}=\begin{bmatrix}\boldsymbol{0} & \boldsymbol{I}\\ -\boldsymbol{M}^{-1}\boldsymbol{K} & -\boldsymbol{M}^{-1}\boldsymbol{C}\end{bmatrix}\begin{bmatrix}\boldsymbol{x}\\ \dot{\boldsymbol{x}}\end{bmatrix}+\begin{bmatrix}\boldsymbol{0}\\ -\boldsymbol{M}^{-1}\boldsymbol{\Lambda}\end{bmatrix}F \tag{10}$$

where F is the band-limited white noise (BLWN) input from a shaker. $\boldsymbol{\Lambda}$ is the loading vector determined by the DOF where the excitation is applied. In the simulations, the input is given in the vertical direction at node 4 (see Fig. 3(b)) aligned with the front panel at the same location as in the experiments. The simulated acceleration output from all nodes on the model is given by $\boldsymbol{Y}$.

$$[\boldsymbol{Y}]=\begin{bmatrix}-\boldsymbol{M}^{-1}\boldsymbol{K} & -\boldsymbol{M}^{-1}\boldsymbol{C}\end{bmatrix}\begin{bmatrix}\boldsymbol{x}\\ \dot{\boldsymbol{x}}\end{bmatrix}+\begin{bmatrix}-\boldsymbol{M}^{-1}\boldsymbol{\Lambda}\end{bmatrix}F \tag{11}$$

$$[\boldsymbol{Y}_s]=[\boldsymbol{Y}(\boldsymbol{\Gamma})] \tag{12}$$

where $\boldsymbol{Y}_s\in\boldsymbol{R}^{k\times 1}$ is the subset of $\boldsymbol{Y}$. $\boldsymbol{\Gamma}$ is the vector determined by the measured DOFs by wireless nodes. $\boldsymbol{Y}_s$ is input to the FDD with peak-picking modal identification algorithm to obtain the natural frequencies and mode shapes in the healthy and damaged conditions. Then, the Level I and Level II damage detection algorithms can be applied with the modal information. The first six mode shapes of the structure are shown in Figs. 4(a)-4(f).

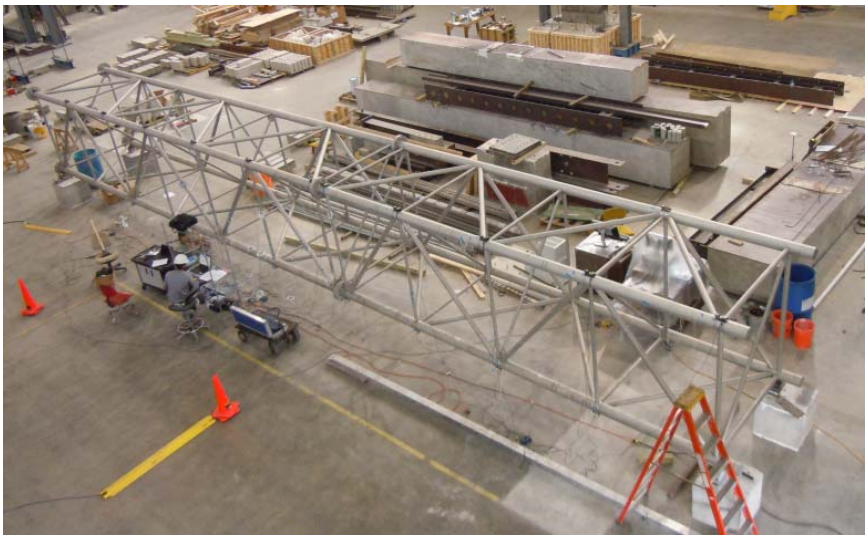

Fig. 2 Full-scale truss structure

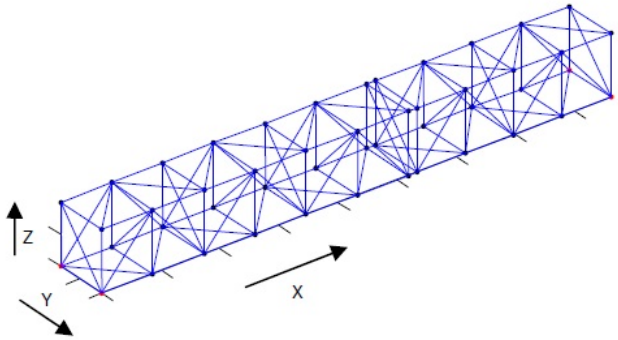

(a) 3D view of the FEM model

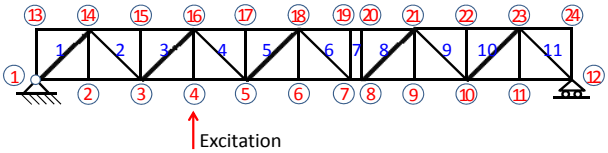

(b) 2D view of the front panel (circled numbers are the node numbers; bare numbers are the bay numbers)

Fig. 3 Numerical model of the truss structure

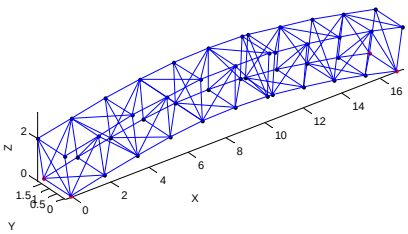

(a) 1st mode (bending mode)

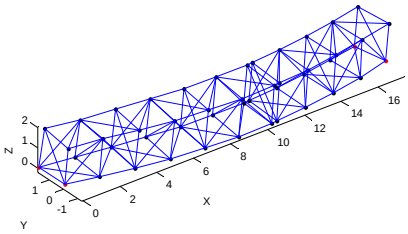

(b) 2nd mode (bending mode)

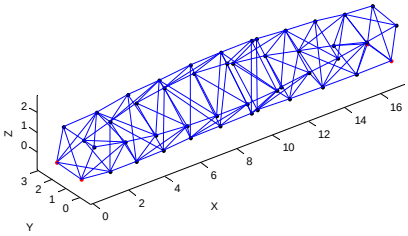

(c) 3rd mode (torsional mode)

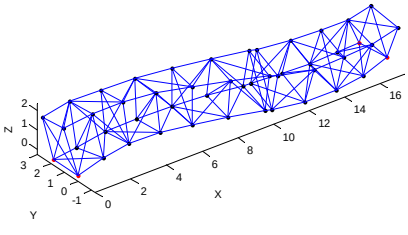

(d) 4th mode (torsional mode)

Continued-

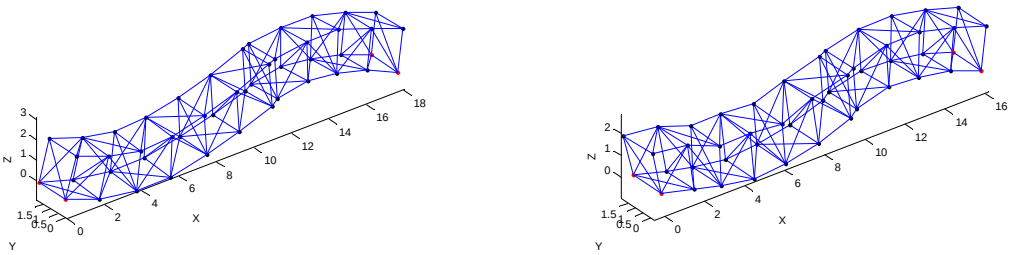

(e) 5th mode (bending mode) (f) 6th mode (bending mode)

Fig. 4 First 6 mode shapes of numerical model

3.2 Damage detection results from simulated tests

Three single damage cases and one multi-damage case are simulated in Matlab. Case N1 simulates that the damage occurs at element 39, which is the diagonal element on the front panel at bay 5; Case N2 simulates that the damage occurs at element 5, which is the horizontal element on the front panel at bay 5. Case N3 simulates that the damage occurs at element 42, which is the diagonal element on the front panel at bay 9. Case N4 simulates that multi-damages occur at elements 39 and 42. The damaged elements are shown in Fig. 5. In the numerical simulation, 1% rms Gaussian noise is added to each channel of the measured data. For Case N1 and Case N2, sensors are assumed to be on the top chord of the front panel for Level I detection. After Level I detection, sleeping sensors in the damaged bay and neighboring bays will wake up for the Level II detection (i.e., the blue square sensors in Figs. 5(a) and 5(b) for Case N1 and Case N2). Similar sensor setup applies for Case N3 and Case N4. The element numbers in Level I & II detection are shown in Fig. 5(b).

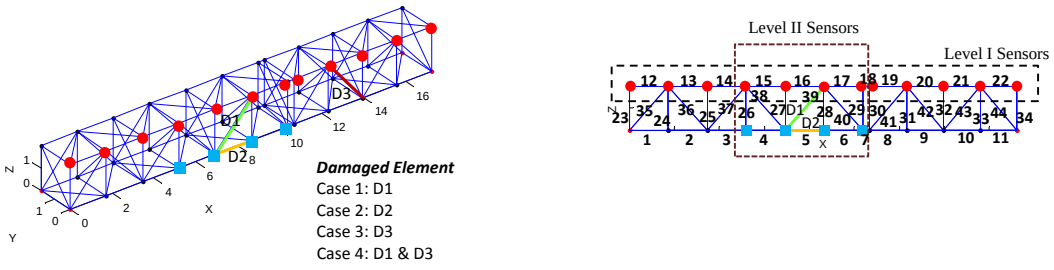

(a) Damaged elements in each case (b) Sensors in Level I & II Detection

Fig. 5 Damage cases and sensors' location in Level I & II Detection

The damage detection results for these four cases are shown in Figs. 6(a)-6(i). The peaks in these plots indicate the damaged bay in Level I detection and the damaged element in Level II detection. A threshold is set up for Level II damage detection to reduce the chance of false positive detection. For these simulated single damage and multi-damage cases, the multi-level damage detection strategy is successful in detecting both the damage bay and the damaged element(s). The multi-level strategy works for these cases on the particular structure. Experimental studies on the full-scale truss with wireless sensors are discussed in the next two sections.

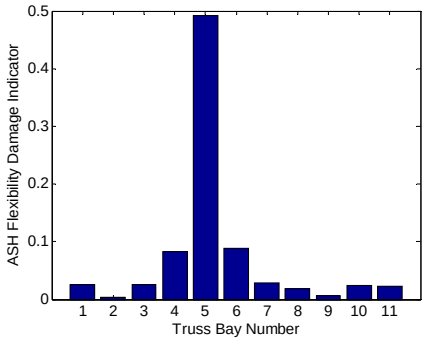

(a) Level I detection for Case N1

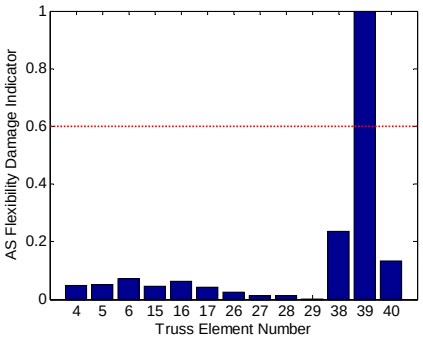

(b) Level II detection for Case N1

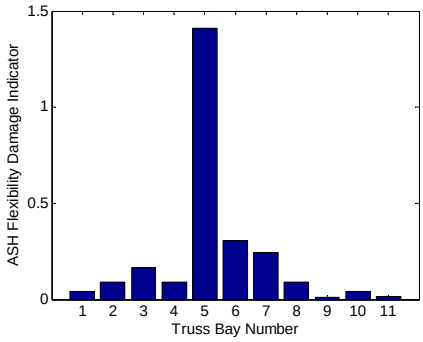

(c) Level I detection for Case N2

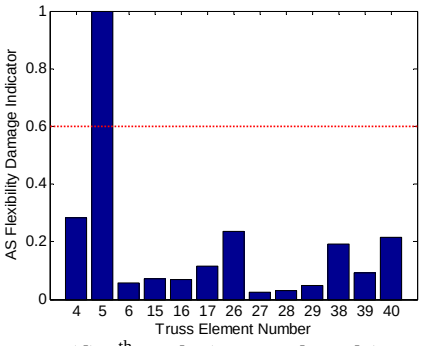

(d) 4th mode (torsional mode)

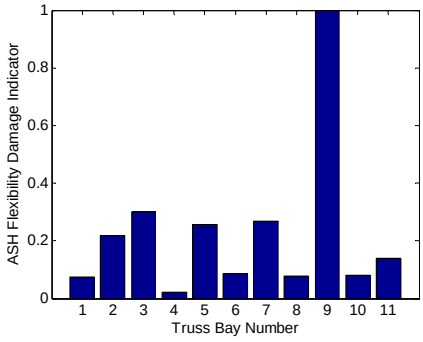

(e) Level I detection for Case N3

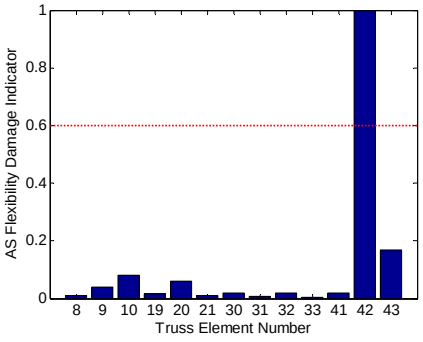

(f) Level II detection for Case N3

Continued-

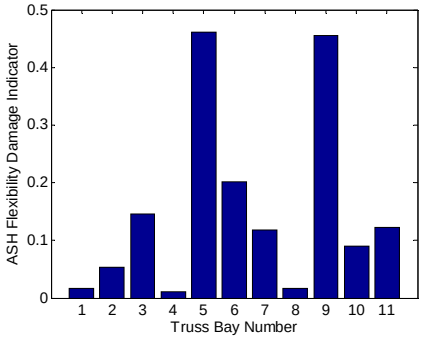

(g) Level I detection for Case N4

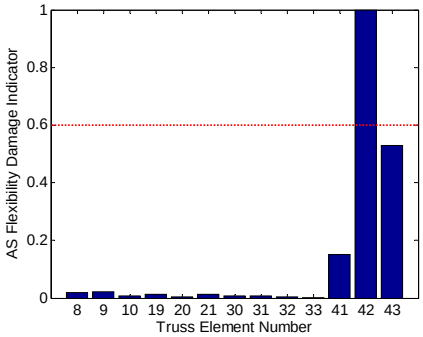

(h) Level II detection for Case N4

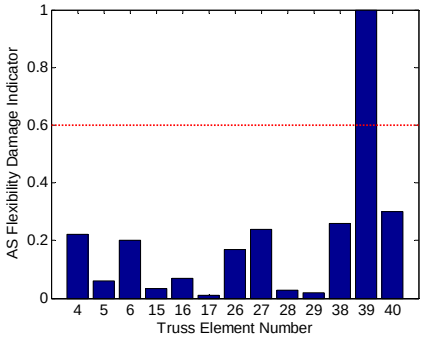

(i) Level II detection for Case N4

Fig. 6 Numerical simulation of Level I and Level II detection

4. Experimental study

Experimental validation of the multi-level damage detection using the WSN is performed on the full-scale highway sign support truss at the Bowen Laboratory for Large-Scale Civil Engineering Research at Purdue University.

4.1 Full-scale experimental setup

The highway sign truss was previously mounted over Interstate I-29 near Sioux City in Iowa to display route message. It has two segments. The two segments are bolted together. The test structure is 17.24 m long, 1.98 m high and 1.83 m wide (Fig. 2). The dimensions of members of the structure are listed in Tables 1 and 2. There are 11 bays in the front panel of the truss, 6 bays in the left segment, 4 bays in the right segment and 1 connection bay. The structure is made of aluminum alloy (6061-T6) with the density of 2.7×10^3 kg/m^3, Young's Modulus of 69.64 GPa and Poisson's ratio of 0.33 (Krishnan 2012, Sun and Dyke 2013). The left ends of the structure are placed on metal plates to simulate pinned support and the right ends of the structure are placed on rollers. An electro-dynamic shaker (VG-100 from Vibration Test Systems) was used to excite the truss in the vertical direction at node 4 (see Fig. 7) of the front panel. The input to the structure is BLWN with bandwidth 0-70 Hz.

Fig. 7 Setup of the shaker

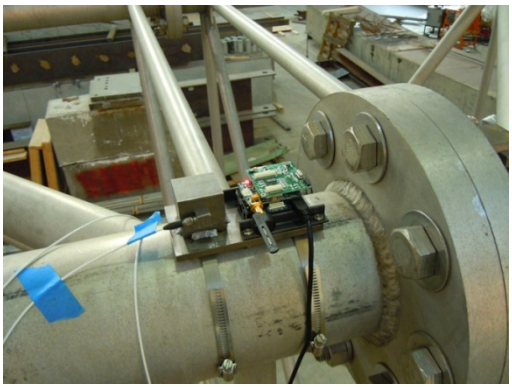

Fig. 8 Setup of the wireless sensors

Table 1 Dimensions of the truss members

Name	Length(m)
Each bay of left segment	1.73
Each bay of right segment	1.64
Connection bay	0.3
Total length of left segment	10.38
Total length of right segment	6.56
Total length of truss	17.24

Table 2 Dimensions of the cross section of members

Name	Outside diameter (cm)	Thickness (cm)
Main cords	15.2	0.83
Diagonal braces	7.6	0.63
End vertical braces	6.4	0.63
All Other members	5.1	0.48

4.2 Wireless sensor network configuration

Nineteen Imote2 wireless nodes with SHM-A sensor board and external antenna (Sim and Spencer 2009) are used in the experiment. Eighteen of the nodes are installed on the highway truss, and among them one node is functioning as manager node. The remaining wireless node is used as

the gateway node at the base station. The gateway node is connected to the base station PC through a USB serial port. The deployment of wireless sensors is shown in Fig. 8. The accelerometers on the SHM-A sensor board are tri-axial accelerometers. Measurement range is ±2g with 0.143 mg resolution in all three directions (ISM400 Datasheet). The microcontroller on Imote2 board has 13 - 416 MHz processor speed, 256 KB SRAM plus 32MB SDRAM which is powerful enough for onboard processing (Imote2 Datasheet). Tinyos (Levis *et al.* 2005) is the embedded operating system on the Imote2 board. ISHMP Toolsuite V3.0 (Spencer and Agha 2011, Jang *et al.* 2010) is used as the software library to implement the distributed FDD algorithm. The sampling frequency of wireless sensors is set to 280Hz with an associated filter cut-off frequency at 70 Hz.

To perform a systematic study of the structure and obtain a complete set of data for the healthy truss case and each damaged truss case, wireless sensors are installed on the bottom and top chords of both the front and the back panel. At the start of a wireless modal identification test, sensor IDs, sampling frequencies, sensing channels and total sample numbers need to be setup, respectively. After sensing raw data, automated modal identification will be conducted following the procedures illustrated in Fig. 1. Instead of modal information, raw sensing data can also be sent to the base station from each node for more in-depth analysis. Two types of wireless network topologies have been used in the tests (see Figs. 9(a) and 9(b)). Topology 1 is for wirelessly collecting raw data and then transmitting it to the base station. Topology 2 is for the distributed modal identification and multi-level damage detection.

4.3 Damage cases considered

Three damage cases are considered in the experimental study. The location of damaged element(s) in each case is shown in Fig. 10(a). First a single cut is created at a diagonal element of bay 5 in the front panel to represent damage Case E1 (see Fig. 10(b)). This case is a full cut through at one end of the diagonal element. The data from the damaged truss are obtained with the WSN. Next, the damaged element is welded together to obtain the healthy truss data (we did this in a reversed order because the damage had already been created in a previous test on this structure).

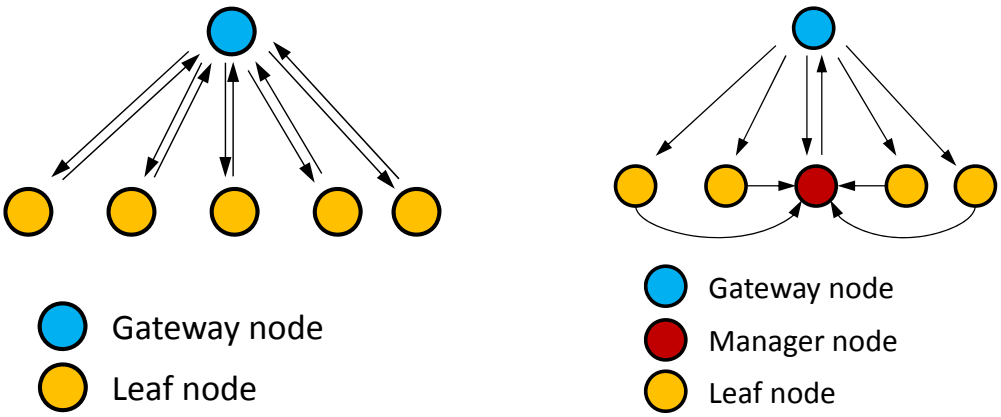

(a) Network Topology 1 (b) Network Topology 2

Fig. 9 Wireless network topology

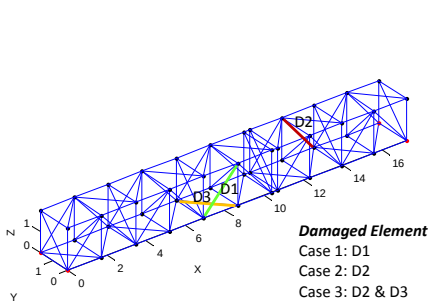

(a) Damaged elements

(b) Damaged element D1 at bay

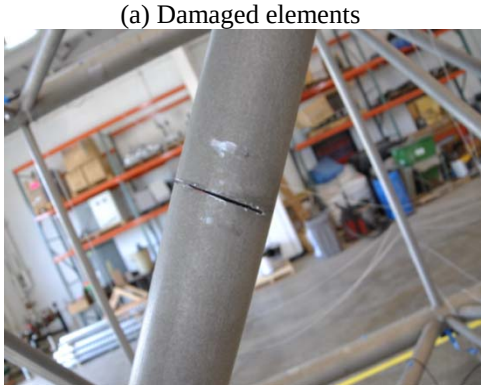

(c) Damaged element D2 at bay 9

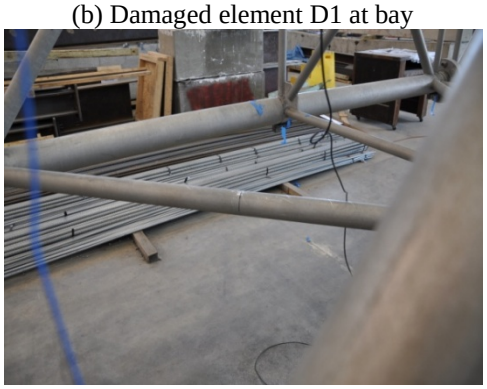

(d) Damaged element D3 at bay 5

Fig. 10 Damage cases for experimental study

A second single damage case (Case E2) is created at the diagonal element of bay 9 in the back panel (see Fig. 10(c)). This case is a half cut through the cross section of the element. The last case (Case E3) is a multi-damage case with damage at bay 9 (the damage created in Case E2) and bay 5 (a half cut at the bottom panel). The multi-level damage detection results for these three cases are discussed in the next section.

5. Experimental results

Raw sensing data from node 5 (Fig. 3(b)) in the vertical direction is shown in Fig. 11(a). The corresponding power spectral density (PSD) plot is shown in Fig. 11(b). The first 10 natural frequencies for the healthy case and different damage cases are listed in Table 3. When damage occurs, structural stiffness generally reduces, and natural frequencies will become lower than the corresponding ones in the healthy structure. This phenomenon is observed from the damaged cases in Table 3. However, for some modes, the natural frequencies increase in the damaged case (i.e. mode 2 of damaged case E2). This may due to the impact of environmental factors such as temperature change or humidity variation.

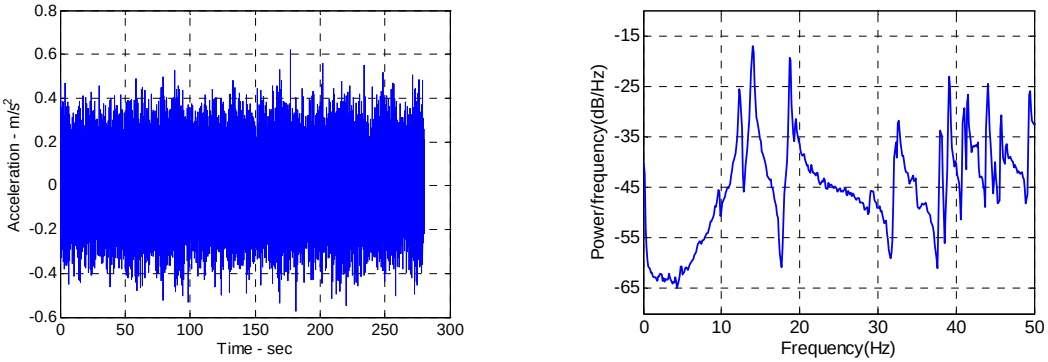

(a) Raw data from wireless node (b) PSD of acceleration output

Fig. 11 Wireless sensor measurements and post-processing

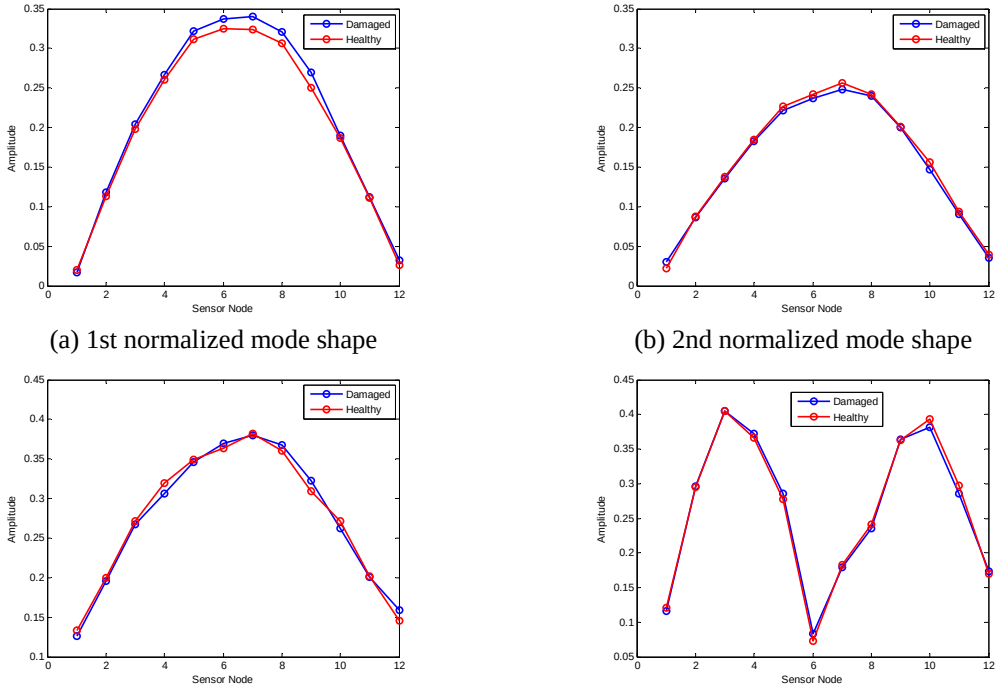

(a) 1st normalized mode shape (b) 2nd normalized mode shape

(c) 3rd normalized mode shape (d) 4th normalized mode shape

Fig. 12 Identified Mode shapes

When implementing the multi-level detection, the mode shapes need to be corresponding to the same mode in the healthy case and damaged case, otherwise misleading detection results will be obtained. The first four corresponding modes in the healthy and damaged structure can be easily identified, and thus used for the multi-level detection. The comparison of first four mode shapes in

healthy and damaged Case E2 is shown in Figs. 12(a)-12(d). The first mode shape is the 1st bending mode in the vertical direction. The 2nd and 3rd mode shapes are torsional modes in the vertical and out-of-plane directions. The 4th mode shape is the 2nd bending mode in the vertical direction. The mode shapes are normalized with the second norm of each mode, respectively. Since the multi-level damage detection strategy utilizes global structural modal information (natural frequencies and mode shapes), if a structural damage did not cause sufficient modal change, the damage detection strategy may not work properly. The sensitivity of the damage detection methods for different damage scenarios are structural dependent and are not the focus of this paper.

Collecting raw sensing data from each node location with topology 1 and performing multi-level damage detection following procedures illustrated in Fig. 1 at the base station is referred as the offline case with experimental data. Using local processing on each leaf node sensor and performing multi-level damage detection following procedures in Fig. 1 is referred as the online case. The multi-level damage detection for Case E1 and Case E3 are using the offline approach. The multi-level damage detection for Case E2 is using both offline and online approach. Offline approaches are conducted more because the raw data can be used for more in-depth analysis of the structure.

The multi-level detections results are shown in Figs. 13(a)-13(j). Figs. 13(a) and 13(b) is for Case E1. The damaged bay 5 has been identified from coarse resolution Level I detection and the damaged element 39 is identified through fine resolution Level II detection. Figs. 13(c) and 13(d) is the Level I detection for case E1 using only healthy truss data at different time to compare with Fig. 13(a). Figs. 13(e)-13(h) is for Case E2. For Case E2, offline results and online results are both available. For Case E2 Level II online detection, only sensors in the damage bay are woken up for the Level II damage detection. So there are fewer element members involved in the online Level II damage detection compared to the offline results.

Table 3 Identified natural frequencies of the structure

	Natural Frequency (Hz)			
Mode	**Healthy**	**Damage Case E1**	**Damage Case E2**	**Damage Case E3**
1	12.71	12.37	12.65	12.65
2	14.70	13.95	14.77	14.83
3	18.73	19.14	18.66	18.66
4	32.88	28.57	32.61	32.54
5	36.16	35.62	36.09	35.27
6	39.31	38.01	38.01	37.05
7	41.02	39.79	40.88	40.95
8	41.49	41.77	41.84	41.84
9	44.02	42.45	44.02	44.16
10	45.73	44.43	44.98	45.66

This explains the differences between Figs. 13(f) and 13(h). Both offline and online results have detected the damage at the element 42. Figs. 13(i)-13(j) is for Case E3, the two damaged elements case. The two damaged bays have been identified in Level I detection even though there is a peak at bay 6. False positive detections in the neighbouring bays of damaged bay in Level I detection have been observed in the authors' previous study. This can be reduced by setting up a proper threshold in Level I detection. The Level II detection result for damaged elements at element 42 is shown in Fig. 13(j). Implementing the multi-level damage detection strategy, single and multi-damage cases have been successfully detected and located through the experimental study.

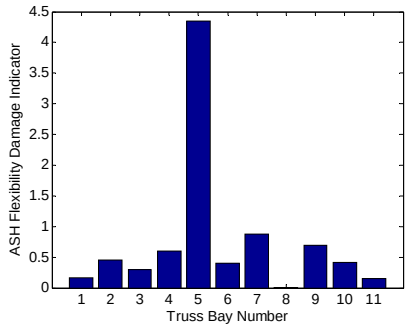

(a) Level I detection for Case E1

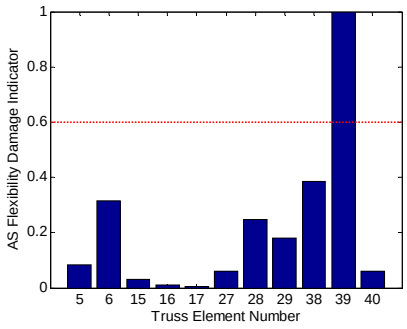

(b) Level II detection for Case E1

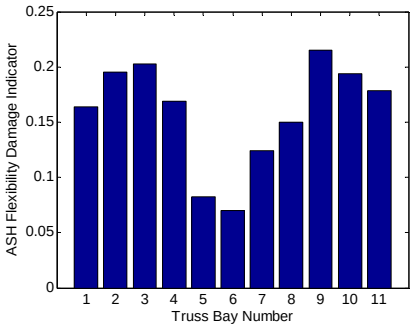

(c) Level I detection for Case E1(healthy)

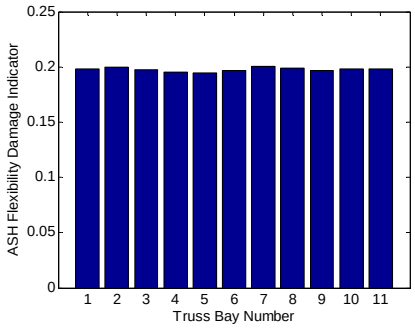

(d) Level I detection for Case E1(healthy)

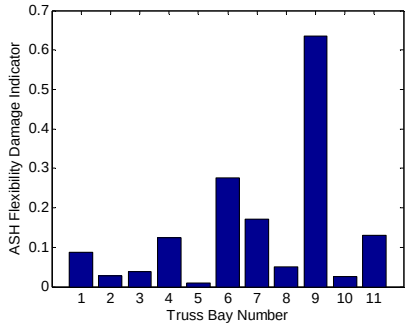

(e) Level I detection for Case E2 (offline)

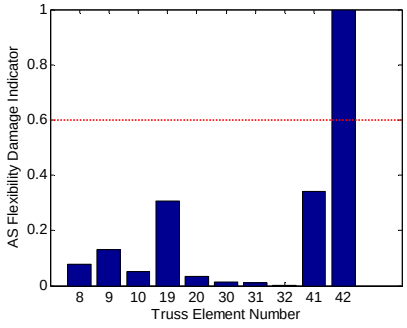

(f) Level II detection for Case E2 (offline)

Continued-

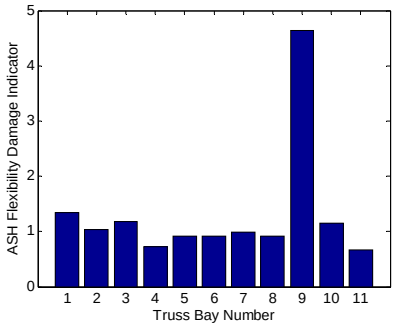

(g) Level I detection for Case E2 (online)

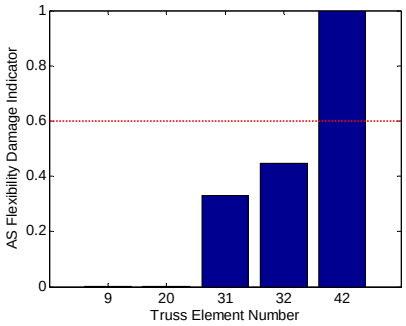

(h) Level II detection for Case E2 (online)

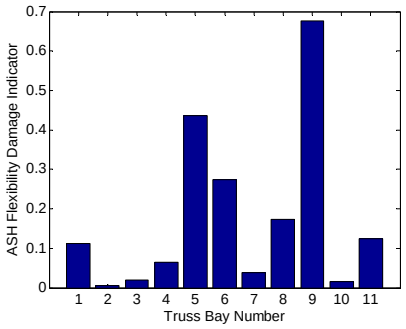

(i) Level I detection for Case E3

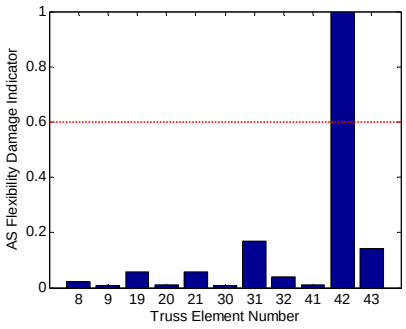

(j) Level II detection for Case E3

Fig. 13 Level I and Level II detection results

It should be mentioned that although modal based approaches for damage detection has been successful in this work and numerous researchers' work (Pandey *et al.* 1991, Talebinejad *et al.* 2011, Meruane and Heylen 2011), there are concerns (Doebling *et al.* 1998, Chang *et al.* 2003) for implementing modal based damage detection algorithms on real world structures, e.g. the impact of environmental variations on the modal properties can lead to false alarms. The authors agree with those concerns and the studies on the robustness and sensitivity of this method will be carried in the follow-up studies using the truss structure.

6. Conclusions

A proposed multi-level damage detection strategy has been successfully implemented on the full-scale highway sign support truss structure. Numerical simulation and experimental tests have been conducted to validate the multi-level detection strategy with WSN. A distributed modal identification algorithm has been implemented with imote2 wireless sensors for online modal identification. The algorithm has been working well with the WSN. The communication load is reduced by about 99% in this implementation using the topology 2 on the imote2 platform with local processing compared to topology 1, which is normally used in traditional approaches. Similarly, the power consumption is also greatly reduced. The damaged bay(s) (Level I) and damaged element(s) (Level II) have been successfully detected for the two single damage cases and one multi-damage case in the experimental study. Data obtained in these experiments have

been uploaded and released on the NEEShub (nees.org) for re-use by other interested researchers (Sun *et al.* 2013).

Acknowledgments

The authors acknowledge support from National Science Foundation under Grant No. CNS-1035748 and Grant No. CNS-1035773. The authors also thank Prof. Robert Connor at Purdue University and Mr. Michael Todsen at Iowa Department of Transportation for helping acquire the truss used in this study. Besides, the authors thank laboratory managers at the Bowen lab for helping moving and assembling the full-scale truss.

References

Bougard, B., Catthoor, F., Daly, D.C., Chandrakasan, A. and Dehaene, W. (2005), "Energy efficiency of the IEEE 802.15.4 standard in dense wireless microsensor networks: modeling and improvement perspectives", *Proceedings of the Design, Automation and Test in Europe Conference and Exhibition*.

Brincker, R., Zhang, L. and Anderson, P. (2001), "Modal identification of output-only systems using frequency domain decomposition", *Smart Mater. Struct*., **10**(3), 441-445.

Castaneda, N., Yan, G. and Dyke, S. (2009), "Evaluation of the performance of a distributed structural health monitoring algorithm for wireless sensing", *Proceedings of the 7th International Workshop on Structural Health Monitoring.* Stanford.

Chang, P.C., Flatau, A. and Liu, S.C. (2003), "Review paper: health monitoring of civil infrastructure", *J. Struct. Health Moni*., **3**, 257-267.

Chintalapudi, K., Fu, T., Paek, J., Kothari, N., Rangwala, S., Caffrey, J., Govindan, R., Johnson, E. and Masri, S. (2006), "Monitoring civil structures with a wireless sensor network", *Internet Computing, IEEE* , 26-34.

Doebling, S.W., Farrar, C.R. and Prime, M.B. (1998), "A summary review of vibration-based damage identification methods", *Shock Vib. Digest* , 91-105.

Dorvash, S., Pakzad, S.N. and Cheng, L. (2013), "An iterative modal identification algorithm for structural health monitoring using wireless sensor networks", *EERI* , **29**(2), 339-365.

Ferrigno, L., Marano, S., Paciello, V. and Pietrosanto, A. (2005), "Balancing computational and transmission power consumption in wireless image sensor networks", *In Virtual Environments, Human-Computer Interfaces and Measurement Systems. Proceedings of the 2005 IEEE International Conference on.*

Gangone, M.V., Whelan, M.J. and Janoyan, K.D. (2009), "Deployment of a dense hybrid wireless sensing system for bridge assessment", *Struct. Infrastruct. E*., doi: 10.1080/15732470802670842 .

Hackmann, G., Guo, W., Yan, G., Lu, C. and Dyke, S. (2010), "Cyber-physical codesign of distributed structural health monitoring with wireless sensor networks", *Proceedings of the 1st ACM/IEEE International Conference on Cyber-Physical Systems (ICCPS '10).*, New York.

Hackmann, G., Sun, F., Castaneda, N., Lu, C. and Dyke, S. (2012), "A holistic approach to decentralized structural damage localization using wireless sensor networks", *Comput. Commun.*, **36**(1)29-41.

He, Z. and Wu, D. (2006), "Resource allocation and performance analysis of wireless video sensors", *Circuits and Systems for Video Technology, IEEE Transactions on* , 590-599.

Imote2 Datasheet, Retrieved from; http://web.univ-pau.fr/~cpham/ENSEIGNEMENT/ PAU-UPPA/RESA -M2/DOC/Imote2_Datasheet.pdf

ISM400 Datasheet, Retrieved from; http://shm.cs.uiuc.edu/files/docs/ISM400_Datasheet.pdf.

Jang, S., Jo, H., Cho, S., Mechitov, K., Rice, J.A., Sim, S.H., Jung, H.J., Yun, C.B., Spencer, B.F. and

Agha, G. (2010), "Structural health monitoring of a cable-stayed bridge using smart sensor technology: deployment and evaluation", *Smart Struct. Syst.*, **6**(5) 439-459.

Kim, S., Pakzad, S., Culler, D. and etc. (2007), *Health Monitoring of Civil Infrastructures Using Wireless Sensor Networks*, In IPSN. ACM.

Krishnan, S.K., Sun, Z., Irfanoglu, A., Dyke, S. and Yan, G. (2011), "Evaluating the performance of distributed approaches for modal identification", *Proceedings of SPIE*, 7981.

Krishnan, S. (2012), *Master dissertation: Establishing a Baseline Damage Index for Reliable Damage Detection: Full Scale Validation*, West Lafayette: Purdue University.

Levis, P., Madden, S., Polastre, J., Szewczyk, R., Whitehouse, K. and Woo, A. (2005), "TinyOS: An operating system for sensor networks", *In Ambient intelligence* , 115-148.

Lynch, J.P. and Loh, K.J. (2006), "A summary review of wireless sensors and sensor networks for structural health monitoring", *Shock Vib. Digest*, **38**(2), 91-130.

Meruane, V. and Heylen, W. (2011), "An hybrid real genetic algorithm to detect structural damage using modal properties", *Mech. Syst. Signal Pr.*, **25**(5), 1559-1573.

Nagayama, T. and Spencer, B.F. (2008), *Structural Health Monitoring Using Smart Sensors*, Newmark Structural Engineering Laboratory. University of Illinois at Urbana-Champaign.

Pakzad, S.N., Fenves, G.L., Kim, S. and Culler, D.E. (2008), "Design and implementation of scalable wireless sensor network for structural monitoring", *J. Infrastruct. Syst.*, **14**(1), 89-101.

Pandey, A.K., Biswas, M. and Samman, M.M. (1991), "Damage detection from changes in curvature mode shapes", *J. Sound Vib*., **145**(2), 321-332.

Sim, S. and Spencer, B. (2009), *Decentralized Strategies for Monitoring Structures using Wireless Smart Sensor Networks*, Newmark Structural Engineering Laboratory. University of Illinois at Urbana-Champaign.

Spencer. (2009), *Wireless Structural Monitoring System Deployed in Korea*, Retrieved from The Department of Civil and Environmental Engineering: http://cee.illinois.edu/node/1022

Spencer, B. and Agha, G. (2011), *Software*, Retrieved from Illinois Structural Health Monitoring Project (ISHMP): http://shm.cs.uiuc.edu/

Spencer, B. and Yun, C. (2010), *Wireless Sensor Advances and Applications for Civil Infrastructure Monitoring*, Newmark Structural Engineering Laboratory. University of Illinois at Urbana-Champaign.

Sun, Z. and Dyke, S.J. (2013), "Evaluation of the SDDLV method for damage detection on a full-scale highway sign support truss", *Proceedings of the 9th International Workshop on Structural Health monitoring 2013.*

Sun, Z., Krishnan, S. and Dyke, S. (2013), "Wireless sensors for dynamic testing of a full scale highway truss: vertical electrodynamic white noise shaker excitation", *Network for Earthquake Engineering Simulation (distributor)*, *Dataset, DOI:10.4231/D3FN10S1W.*

Talebinejad, I., Fischer, C. and Ansari, F. (2011), "Numerical evaluation of vibrationbased methods for damage assessment of cable stayed bridges", *Comput.- Aided Civil Infrastruct. Eng.*, **26** (3), 239-251.

Xu, N., Rangwala, S., Chintalapudi, K.K., Ganesan, D., Broad, A., Govindan, R., *et al.* (2004), "A wireless sensor network for structural monitoring", *Proceedings of the 2nd international conference on Embedded networked sensor systems*.

Yan, G., Duan, Z. and Ou, J. (2010), "Damage detection for beam structures using an angle-between-string-and-horizon flexibility matrix", *Struct. Eng. Mech*., **36**(5), 643-667.

Yan, G., Duan, Z. and Ou, J. (2009), "Damage detection for truss or frame structures using an axial strain flexibility", *Smart Struct. Syst*., **5**(3), 291-316.

Yan, G., Dyke, S. and Irfanoglu, A. (2011), "Experimental validation of a damage detection approach on a full-scale highway sign support", *Mech. Syst. Signal Pr*., **28**, 195-211.

Zhang, Y., Tien, D. and Xu, W. (2013), "The analysis of energy consumption and measurement of wireless mesh network", *Proceedings of the 8th International Conference on Information Technology and Applications (ICITA 2013)*.

Zhu, D., Guo, J., Cho, C., Wang, Y. and Lee, K. (2012), "Wireless mobile sensor network for the system identification of a space frame bridge", *Mechatronics, IEEE/ASME Transactions on*, 499-507.

Zimmerman, A.T., Shiraishi, M., Swartz, R.A. and Lynch, J.P. (2008), "Automated modal parameter estimation by parallel processing within wireless monitoring systems", *J. Infrastruct. Syst.*, **14**(1), 102-113.
Zimmerman, A.T., Swartz, R.A. and Lynch, J.P. (2008), "Automated identification of modal properties in a steel bridge instrumented with a dense wireless sensor network", *Bridge Maintenance, Safety, Management, Health Monitoring and Informatics*, 1608-1615.

BS